Electronic Supplementary Material (ESI) for CrystEngComm.

Surface-oxidized titanium diboride as cocatalyst on hematite photoanode for solar water splitting

Qiannan Wu, [a] *Xiao Liang,* [a] *Hui Chen,* [a] *Lan Yang,* [a] *Tengfeng Xie,* [b,*] *Xiaoxin Zou,* [a,*]

[a] State Key Laboratory of Inorganic Synthesis and Preparative Chemistry, College of Chemistry, Jilin University, Changchun 130012, P. R. China,

[b]College of Chemistry, Jilin University, Changchun 130012, People's Republic of China.

*Corresponding authors. E-mail: xxzou@jlu.edu.cn (X. Zou)

1. EXPERIMENTAL SECTION

1.1. Characterizations. The X-ray diffraction (XRD) patterns were recorded by a Bruker D8 Advance. The scanning electron microscope (SEM) images were obtained with a JEOL JSM 6700F electron microscope. The transmission electron microscope (TEM) images were obtained with a Philips-FEI Tecnai G2S-Twin microscope equipped with a field emission gun operating at 200 kV. The X-ray photoelectron spectroscopy (XPS) was performed on an ESCALAB 250 X-ray photoelectron spectrometer with a monochromatic X-ray source (Al Kα hυ = 1486.6 eV). The UV-vis absorption spectrum of the samples was obtained by an UV-vis-NIR spectrophotometer (Shimadzu UV-3600). The work function (WF) measurement was carried out on a Kelvin probe instrument (SKP 5050, KP Technology Ltd, UK). SPV and TPV measurements were conducted on home-made systems.

1.2. Photophysical Characterizations.

Surface photovoltage spectrum (SPV) measurements were conducted on home-made systems to investigate the photogenerated charge behaviors. Briefly, the monochromatic light was provided by a 500 W xenon lamp (LSH-X500, Zolix) and a grating monochromator (Omni-5007, Zolix). Acquisition of the photovoltage signals was realized by a lock-in amplifier (SR830-DSP, Stanford) with a light chopper (SR540, Stanford) and a computer. Normally, a low chopping frequency of 23 Hz was employed in the measurement.

Transient photovoltage spectrum (TPV) measurement was also carried out on home-made systems. In short, the testing systems were constituted of a third-harmonic Nd:YAG laser (Q-smart 450,Quantel), a 500 MHz digital phosphor oscilloscope (TDS 5054, Tektronix) and a photovoltage cell. It was noted that the wavelength and intensity of the laser pulse were 355 nm and 100 μJ, respectively.

Photoluminescence spectrum (PL) was recorded by Horiba FluoroMax-4 under an excitation range from 500 nm to 800 nm

1.3. PEC measurements. The PEC measurements were recorded by a CHI 660E basing on the three-electrode system, The obtained photoanodes were used as working electrode, Ag/AgCl (3 M KCl) was used as reference electrode, and platinum wire was used as counter electrode. The light source is a 300 W xenon lamp (Perfect-Light). The light intensity was adjusted by an irradiatometer (FZ-A, Photoelectric Instrument Factory of Beijing Normal University). Additionally, the illuminated area of photoanode was 0.283 cm^2.

The linear sweep voltammetry (LSV) was measured to obtain the current density vs. applied potential curve, and the potential in this work was converted to the RHE according the Nernst equation:

$$E_{RHE} = E_{Ag/AgCl} + 0.059pH + E^{\theta}_{Ag/AgCl}$$

The plots of the applied bias photon-to-current efficiency (ABPE) as a function of applied bias were obtained by the equation:

$$ABPE = J_{ph} \times (1.23 - E)/P_{light,}$$

here J_{ph} was the photocurrent density (mA/cm^2), P_{light} was the light power intensity (mW/cm^2), and E was the applied bias (V).

The injection efficiency (η_{inj}) was calculated using the following equation:

$$\eta_{inj} = J_{PEC}/J_{H2O2}$$

where J_{PEC} is photocurrent density obtained in KOH electrolyte, J_{H2O2} is the photocurrent obtained in KOH/H_2O_2 electrolyte.

The incident photon-to-current efficiency (IPCE) was measured with the help of monochromator, which was calculated with the following equation:

$$IPCE = \frac{1240 \times J}{\lambda \times P_{mono}}$$

where J was the measured photocurrent density, λ and P were the incident light wavelength and power density, respectively.

The Electrochemical Impedance Spectroscopy (EIS) was measured with a frequency range of 10^5 Hz-0.05 Hz in order to research the charge transport dynamics of the photoanodes. The Mott-Schottky (M-S) plots were carried out in dark condition

at a frequency of 1000 Hz. Accumulated charge density measurements were obtained by integration of the initial current spike at the moment of light close-open conversion.

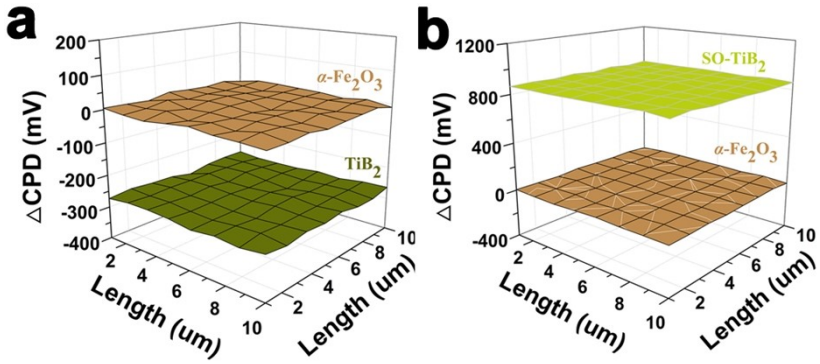

Figure S1. The WF measurement of as-prepared samples.

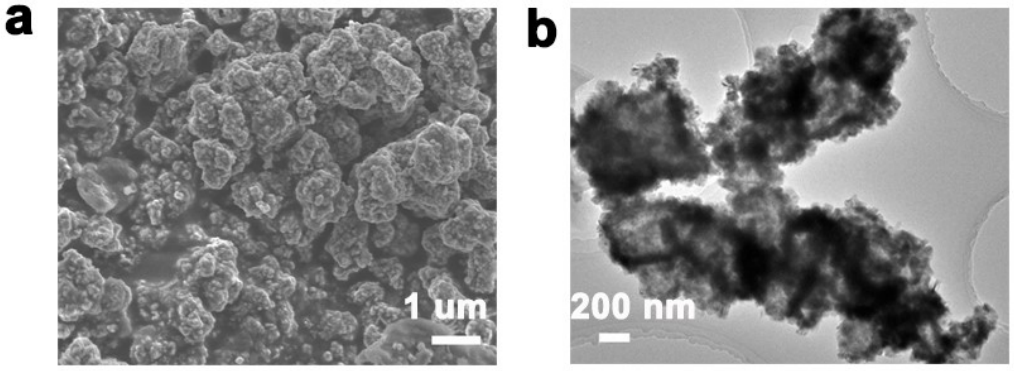

Figure S2. The SEM and TEM image of TiB_2.

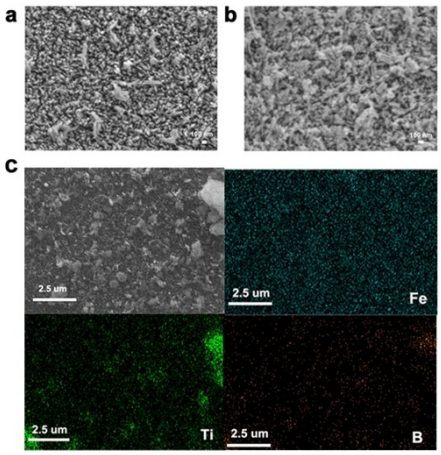

Figure S3. The top-view images of α-Fe_2O_3 photoanode (a) and α-Fe_2O_3/SO-TiB_2 photoanode (b), (c) The elemental mapping for α-Fe_2O_3/SO-TiB_2 photoanode.

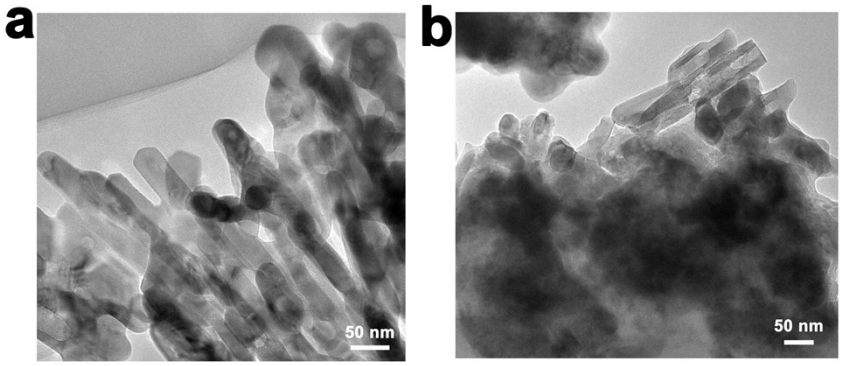

Figure S4. The TEM images of α-Fe_2O_3 photoanode (a) and α-Fe_2O_3/SO-TiB_2 photoanode (b).

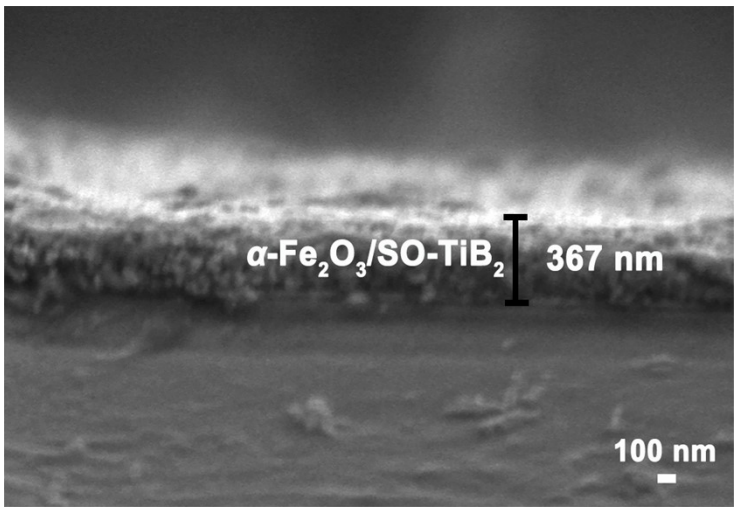

Figure S5. The cross-sectional image of α-Fe_2O_3/SO-TiB_2 photoanode.

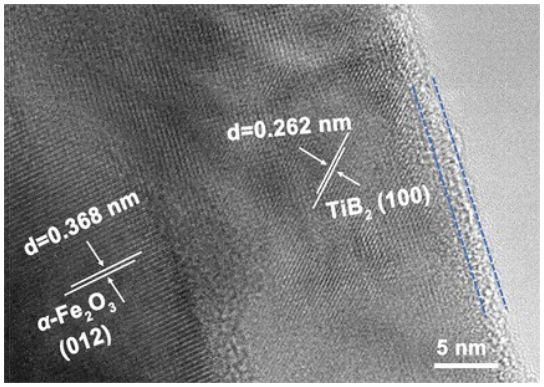

Figure S6. The HRTEM image of α-Fe_2O_3/SO-TiB_2 photoanode.

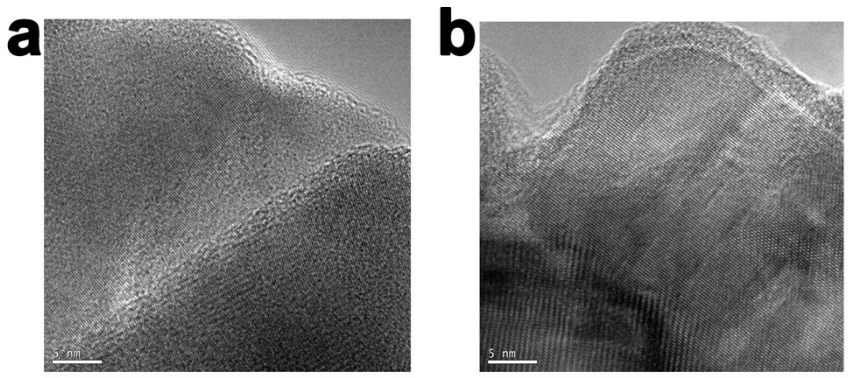

Figure S7. The TEM images of powder TiB_2 (a) and powder SO-TiB_2 (b).

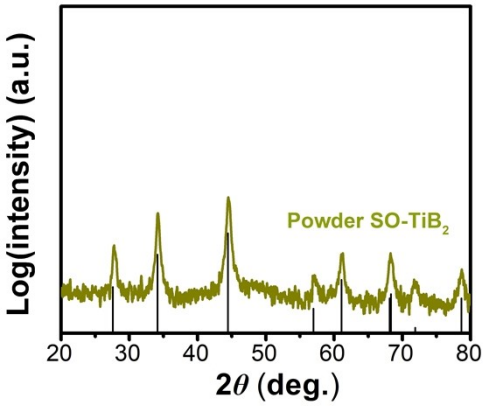

Figure S8. XRD pattern of powder SO-TiB_2.

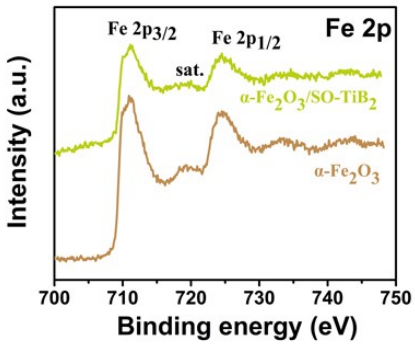

Figure S9. Fe 2p XPS spectra of α-Fe_2O_3 and α-Fe_2O_3/SO-TiB_2.

Table S1 Comparison of the other reported α-Fe_2O_3 photoanodes for PEC water splitting under AM 1.5G illumination

Photoanodes	Photocurrent density	Electrolyte	Light intensity	Reference
Cu@α-Fe_2O_3-Vo-pn photoanode	2.49 mA/cm^2 at 1.23 V vs. RHE	1 M KOH	100 mW/cm^2	1
Fe_2O_3/$FePO_4$/FeOOH	2.02 mA/cm^2 at 1.23 V vs. RHE	1 M NaOH	1000 mW/cm^2	2
α-Fe_2O_3-450	1.035 mA/cm^2 at 1.23 V vs. RHE	1 M KOH	100 mW/cm^2	3
CoPi/Zr-$ZnFe_2O_4$/Fe_2O_3	0.780 mA/cm^2 at 1.23 V vs. RHE	1 M NaOH	100 mW/cm^2	4
In_2S_3/F-Fe_2O_3	2.21 mA/cm^2 at 0.8 V vs. SCE	1 M KOH	100 mW/cm^2	5
α-Fe_2O_3/SO-TiB_2	2.0 mA/cm^2 at 1.23 V vs. RHE	1 M KOH	100 mW/cm^2	in this work

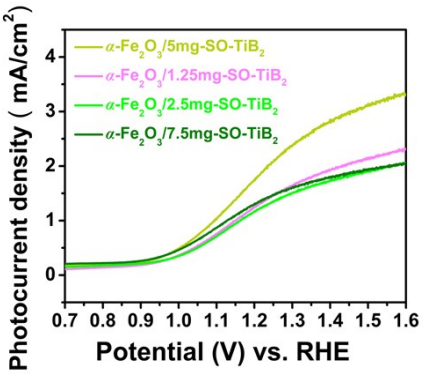

Figure S10. LSV curves of TiB_2-modified photoanodes with different loading.

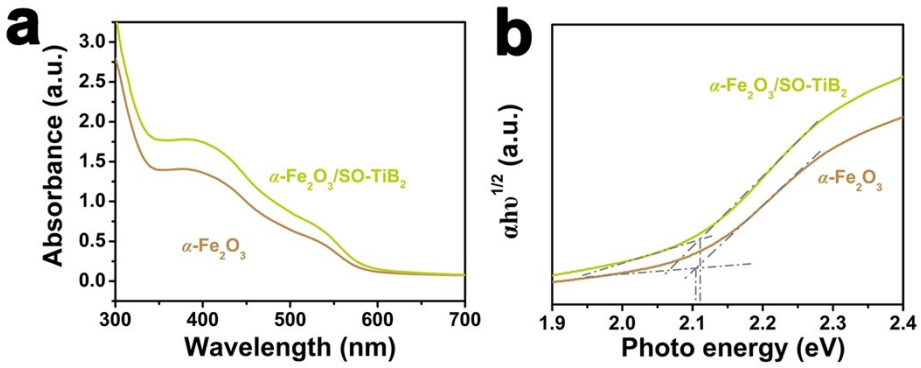

Figure S11. The light absorption (a) and the corresponding Tauc's plots (b) of α-Fe_2O_3 and α-Fe_2O_3/SO-TiB_2.

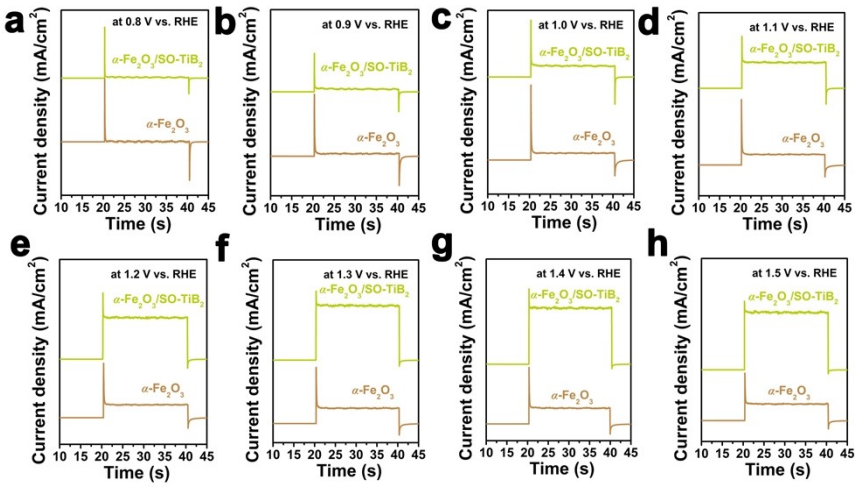

Figure S12. The transient current spikes of photoanode at different potentials.

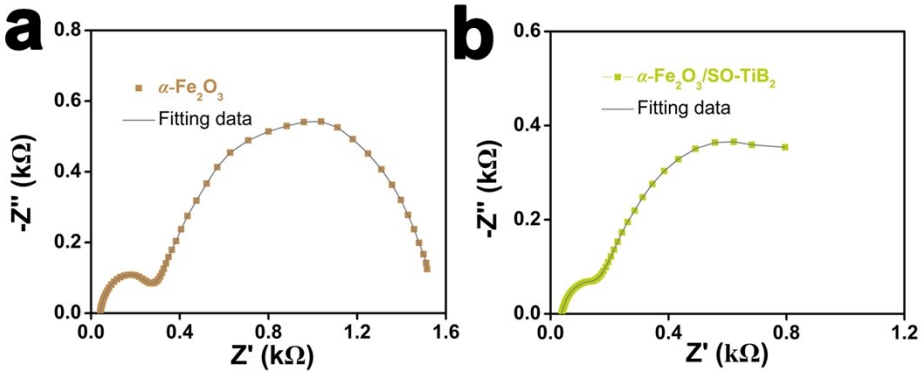

Figure S13. The fitted datas of α-Fe_2O_3 (a) and α-Fe_2O_3/SO-TiB_2 (b).

Table S2. The fitted results according from the Nyquist plots

	R_1 (Ω)	R_2 (Ω)
α-Fe_2O_3	254.3	1242
α-Fe_2O_3/SO-TiB_2	144	851

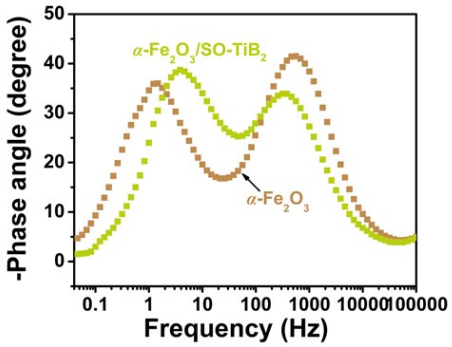

Figure S14. Bode plots of samples at 1 V vs. RHE under AM 1.5 G illumination.

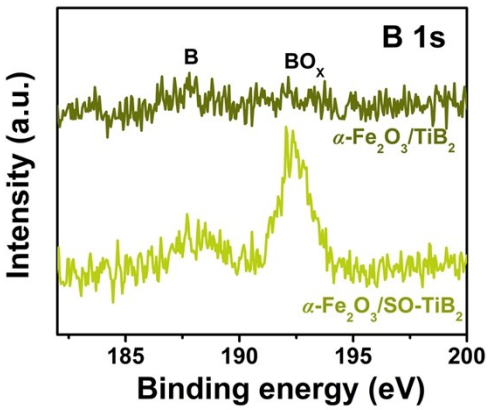

Figure S15. B 1s XPS spectra of α-Fe_2O_3/TiB_2 and α-Fe_2O_3/SO-TiB_2.

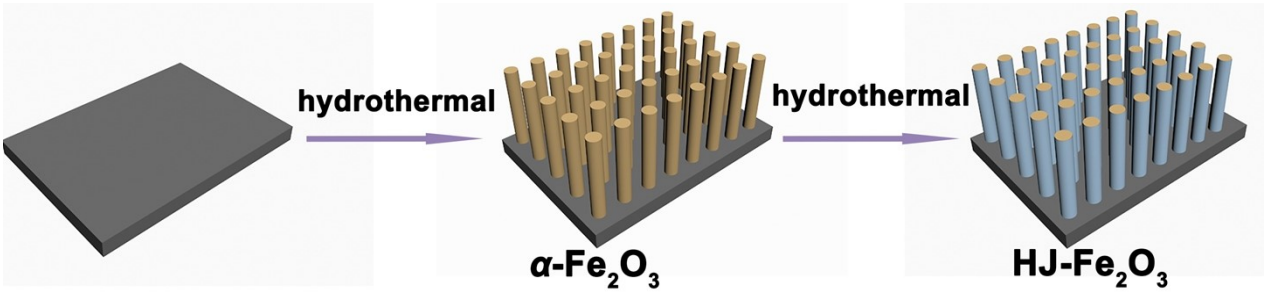

Figure S16. The schematic diagram of the preparation process of HJ-Fe_2O_3.

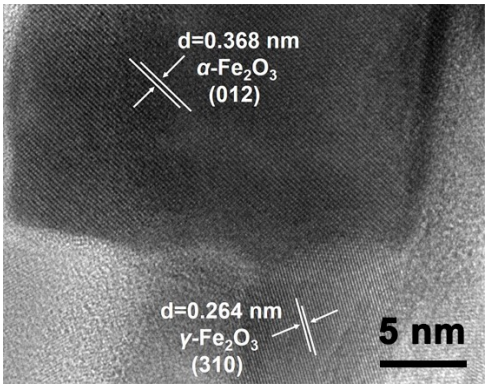

Figure S17. The TEM image of HJ-Fe_2O_3.

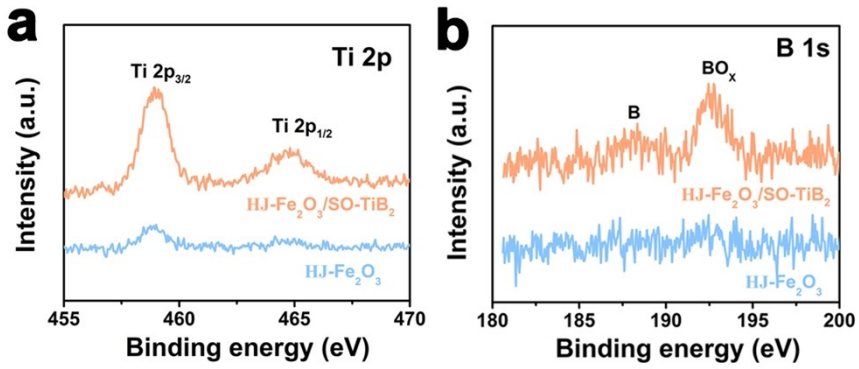

Figure S18. Ti 2p XPS spectra (a) and B 1s XPS spectra (b) of HJ-Fe_2O_3 and HJ-Fe_2O_3/SO-TiB_2.

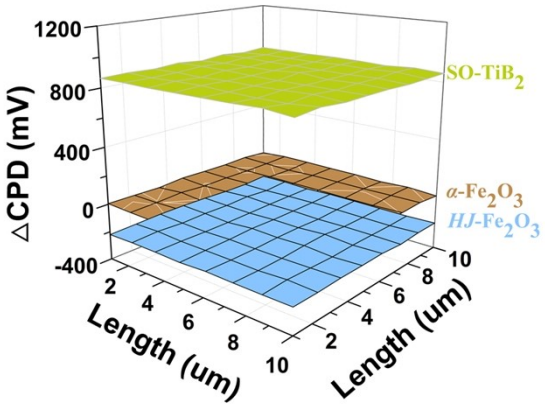

Figure S19. The WF measurement of HJ-Fe_2O_3, SO-TiB_2 and α-Fe_2O_3.

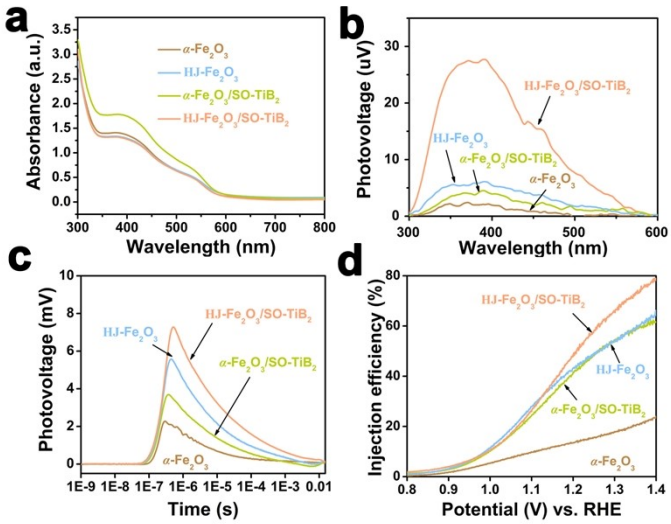

Figure S20. The light absorption (a), the SPV (b), the TPV (c) and the injection efficiency (d) of photoanode.

Notes and references

1. H. Wang, Y.-l. Hu, G.-L. Song and D.-J. Zheng, *Chemical Engineering Journal*, 2022, **435**, 135016.
2. Q. Wang, X. Zong, L. Tian, Y. Han, Y. Ding, C. Xu, R. Tao and X. Fan, *ChemSusChem*, 2022, e202102377.
3. M. Ai, X. Li, L. Pan, X. Xu, J. Yang, J.-J. Zou and X. Zhang, *Chemical Engineering Science*, 2022, **250**, 117397.
4. S. Kim, P. Anushkkaran, W.-S. Chae, S. H. Choi, M. Kumar, M. Cho, M. A. Mahadik, H. H. Lee and J. S. Jang, *ACS Applied Energy Materials*, 2021, **5**, 915-929.
5. H. Chai, L. Gao, P. Wang, F. Li, G. Hu and J. Jin, *Applied Catalysis B: Environmental*, 2022, **305**, 121011.